UNDERSTANDING THE FIELD DEPENDENCE OF SURFACE RESISTANCE IN NITROGEN-DOPED CAVITIES *

P. N. Koufalis†, D. Gonnella, M. Liepe, J. T. Maniscalco, I. Packtor
CLASSE, Cornell University, Ithaca, NY 14853

Abstract

An important limiting factor in the performance of superconducting radio frequency (SRF) cavities in medium and high field gradients is the intrinsic quality factor and, thus, the surface resistance of the cavity [1]. The exact dependence of the surface resistance on the magnitude of the RF field is not well understood. We present an analysis of experimental data of LT1-3 and LT1-4, 1.3 GHz single-cell nitrogen-doped cavities prepared and tested at Cornell [2]. Most interestingly, the cavities display anti-Q slopes in the medium field region (i.e. R_s decreases with increasing accelerating field). We extract the temperature dependent surface resistances of the cavities, analyze field dependencies, and compare with theoretical predictions. These comparisons and analyses provide new insights into the field dependence of the surface resistance and improve our understanding of the mechanisms behind this effect.

CAVITY PREPARATION

Two single-cell, 1.3 GHz, TESLA-shaped cavities (LT1-3 and LT1-4) were nitrogen-doped using the following preparation methods inspired by [3].

1. 150 μm vertical electropolish (VEP)
2. 800 °C bake
   (a) 3 hours in vacuum
   (b) 20 minutes in 60 mTorr of N_2 gas
   (c) 30 minutes in vacuum
3. LT1-3 received a 12 μm VEP
4. LT1-4 received a 24 μm VEP

After preparation, the cavities were RF tested vertically in cw mode. The quality factor, Q_0, was measured at various temperatures and accelerating fields. The surface resistance, R_s, was then calculated from the Q_0 data. The temperature dependent part of the surface resistance, R_{BCS}, was then extracted from the R_s values. Figure 1 summarizes the R_{BCS} data obtained from measurements.

DATA ANALYSIS AND MODELING

We begin our analysis of the data using an approximate model describing the relation between the the Bardeen-Cooper-Schrieffer resistance, R_{BCS}, temperature, T, and two model parameters.

$$R_{BCS} = \frac{A}{T} e^{-\epsilon/k_B T} \tag{1}$$

The pre-exponential factor, A, and the effective energy gap, ϵ, are the model parameters which in general are assumed to be functions of E_{acc}. Letting both parameters vary simultaneously with the accelerating field resulted in a sloppy fit of the data. Because of this, we let only one parameter vary while holding the other fixed. In this way, we were able to independently extract the field dependence of each model parameter. Naturally, this leads to two possibilities, summarized in Eqs. 2 and 3:

$$R_{BCS}(E_{acc}) = \frac{A(E_{acc})}{T} e^{-\epsilon/k_B T} \tag{2}$$

$$R_{BCS}(E_{acc}) = \frac{A}{T} e^{-\epsilon(E_{acc})/k_B T} \tag{3}$$

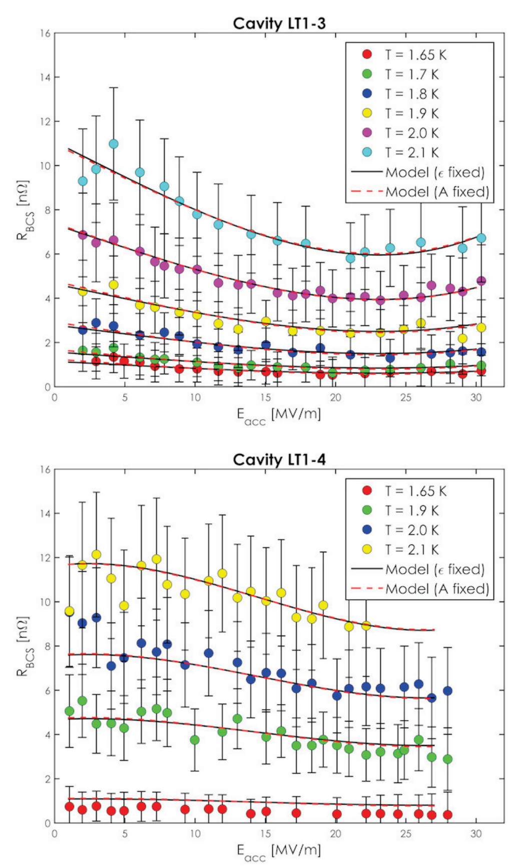

Figure 1: R_{BCS} vs. E_{acc} at various temperatures with both models from Eq. 2 and 3 plotted against the measurement data.

* Work supported by NSF grant PHYS-1416318
† pnk9@cornell.edu

Copyright © 2015 CC-BY-3.0 and by the respective authors

ISBN 978-3-95450-178-6

It turns out that either model works well in modeling the data, as can be seen in Fig. 1.

The data points in Fig. 2 were obtained by fitting R_{BCS} plotted as a function of T at fixed field values with one of the parameters optimized and fixed. The optimal value for the fixed parameter was found via a minimization of a χ^2 test. Fits were then performed in which the free parameter was optimized resulting in the field dependencies shown in Fig. 2. The model curves were obtained by optimizing both the fixed and free parameter by minimizing the sum of the squared error between a cubic polynomial fit of the R_{BCS} vs. E_{acc} data and the model.

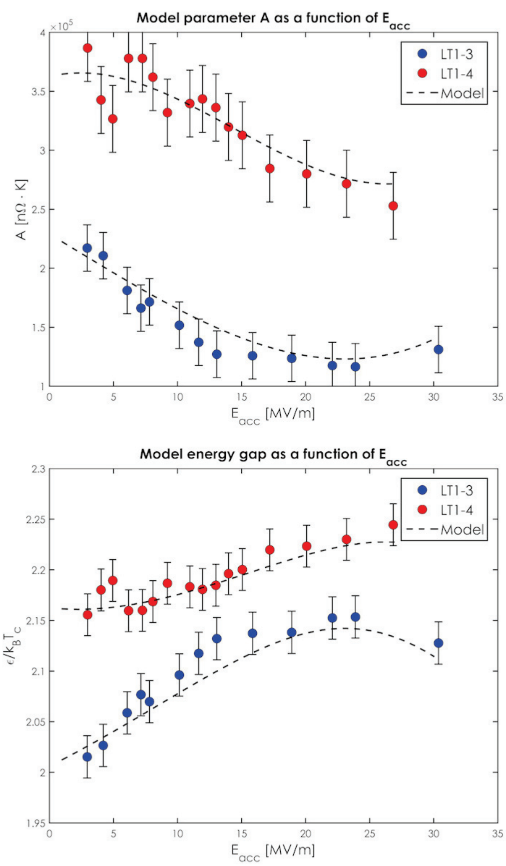

Figure 2: **Top:** The pre-exponential factor A vs. E_{acc}. The model curves are also included. The effective energy gap is fixed. **Bottom:** Effective quasi-particle energy gap, ϵ/k_BT_c plotted against E_{acc} along with the corresponding model (T_c = 9.28 K for LT1-3 and 9.22 K for LT1-4). The pre-exponential factor A is fixed.

The anti-Q slope can be explained by assuming an increase in the effective energy gap with increasing field. However, it can equally well be explained by an assumed decrease in the pre-exponential factor A with increasing field. We further investigated this behavior with an additional analysis using a model based on material parameters of the cavities utilizing the SRIMP BCS code [4].

MEAN FREE PATH AND ENERGY GAP MODEL

The measured change in resonant frequency was used to determine the change in penetration depth, λ. The $\Delta\lambda(T)$ and $R_{BCS}(T)$ data at low field was fit using the SRIMP code to extract a low-field value for the mean free path ℓ, effective quasi-particle energy gap ϵ, and critical temperature T_c [5]. Then, R_{BCS} vs. E_{acc} data was fit holding either ϵ or ℓ constant at the previously extracted value and varying the other parameter as a function of field. The model with ϵ=$\epsilon(E_{acc})$ permits a good fit the experimental data while varying ℓ and keeping ϵ fixed was found to be insufficient to adequately predict the observed strong reduction in R_{BCS} in the medium-field region. This is attributable to the fact that the mean free path of the cavities is already near the minimum of R_{BCS} in the R_{BCS} vs. ℓ curve predicted by BCS theory and is insufficient to change R_{BCS} significantly enough to explain this behavior (i.e. R_{BCS} varies slowly with ℓ). Figure 3 demonstrates that assuming a field dependent effective energy gap while holding ℓ at its constant measured low-field value produces a good fit to the data. The solid lines represent the model whereas the circles are the measured data values. The results so far indicate a field dependency of the effective gap (i.e. a field dependency on the density of states) on the accelerating field which is responsible for the reduction of R_{BCS} in the medium-field region.

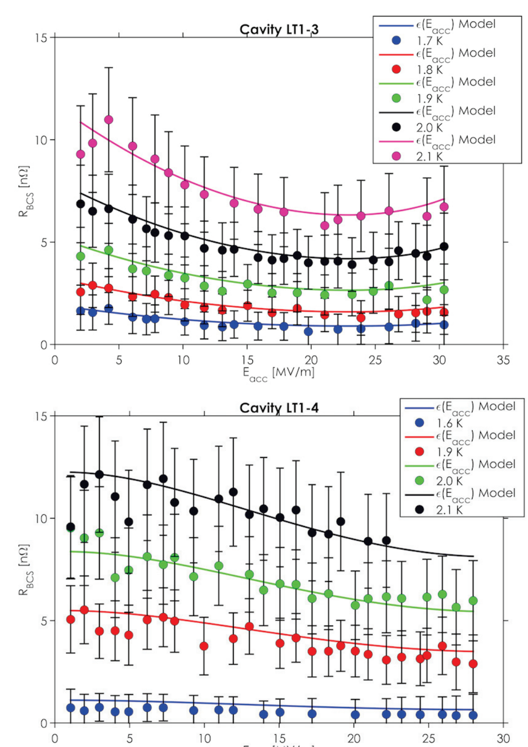

Figure 3: R_{BCS} vs. E_{acc} with model curves letting the effective energy gap vary while assuming a fixed mean free path using SRIMP to model BCS theory.

ISBN 978-3-95450-178-6

Copyright © 2015 CC-BY-3.0 and by the respective authors

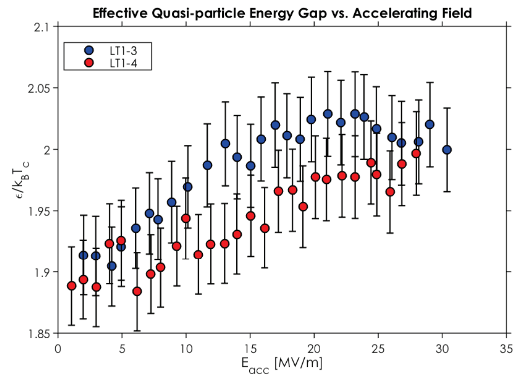

Figure 4: Effective quasi-particle energy gap vs. E_{acc} using SRIMP to extract the effective gap values.

FIELD DEPENDENT BCS SIMULATION

This simulation uses a field dependent derivation of Mattis-Bardeen theory of the RF surface impedance with moving Cooper pairs to model for the field dependence of the surface resistance [6]. Using material parameters ϵ, ℓ, and T_c derived from the BCS fitting done at low RF fields in the previous section, we calculated the field dependent surface resistance based on this theory to compare to the measured values. The simulation agrees reasonably well with experiment, though it deviates somewhat in the low and high field regions at higher temperatures (Fig 5). This implies a simplification in the theory or other field dependent effects that are not included in the model.

CONCLUSION

We have shown that the effective energy gap's field dependence is a likely candidate for the observed strong reduction in R_{BCS} in the medium-field region in impurity-doped SRF cavities. Further investigation is needed to find the exact dependence of the effective energy gap on the field as well as the physical mechanism which causes this dependency. The field dependent theoretical model based on modified Mattis-Bardeen theory needs improvement to accurately describe the observed field dependence of nitrogen-doped cavities. A more complete theory exists which could potentially more precisely explain the observed field dependence [7].

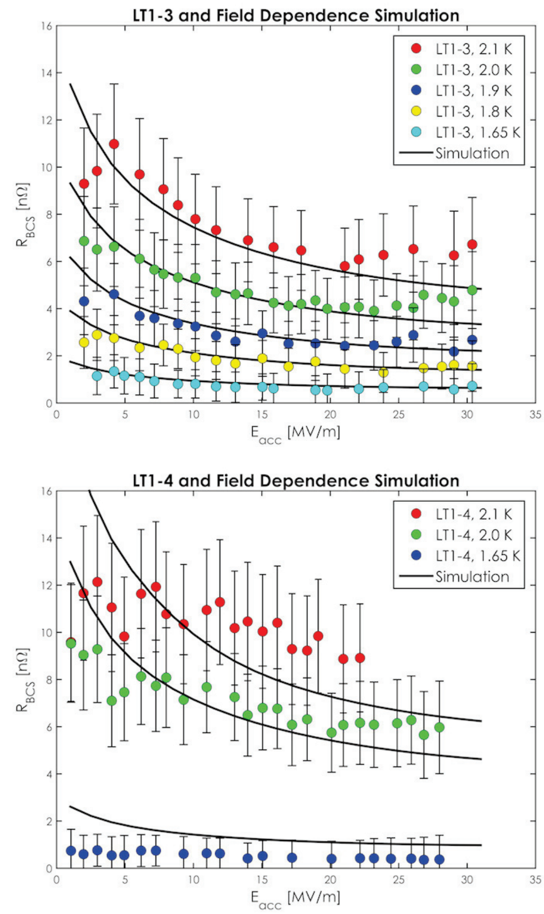

Figure 5: R_{BCS} vs. E_{acc} with field dependent BCS simulation based on [6] using material parameters obtained at low fields. Simulation agrees well with the experimental data for LT1-3 but disagrees with data from LT1-4.

REFERENCES

[1] H. Padamsee, J. Knobloch, and T. Hays. *RF Superconductivity for Accelerators*. Wiley-VCH, 2nd edition, 2008.

[2] D. Gonnella, M. Ge, F. Furuta, and M. Liepe. Nitrogen treated cavity testing at cornell. *Proceedings of LINAC 2014*, 2014.

[3] A. Grassellino, A. Romanenko, D. Sergatskov, O. Melnychuk, Y. Trenikhina, A. Crawford, A. Rowe, M. Wong, T. Khabiboulline, and F. Barkov. Nitrogen and argon doping of niobium for superconducting radio frequency cavities. *Supercond. Sci. Technol.*, 26(102001), 2013.

[4] J. Halbritter. Fortran-program for the computation of the surface impedance of superconductors. Technical Report (3/70-6), KAROLA-OA-Volltextserver des Forschungszentrums Karlsruhe, 1970.

[5] D. Gonnella and M. Liepe. High q0 studies at cornell. *Proceedings of SRF13*, 2013.

[6] B. P. Xiao, C. E. Reece, and M. J. Kelley. Superconducting surface resistance under radiofrequency field. *Physica C*, 490(0):26–31, 2013.

[7] A. Gurevich. Reduction of dissipative nonlinear conductivity of superconductors by static and microwave magnetic fields. *Phys. Rev. Lett.*, 113(087001), 2014.

Copyright © 2015 CC-BY-3.0 and by the respective authors